DOI: 10.1002/zaac.201200455

Low-Temperature Synthesis, Characterization, and Stability of Spinel-Type Li_2NiF_4 and Solid-Solutions $Li_2Ni_{1-x}Co_xF_4$

Julia Kohl,[a] Suliman Nakhal,[a] Noel Ferro,[b] Patrick Bottke,[c] Martin Wilkening,[c] Thomas Bredow,[b] Paul Heitjans,[d] and Martin Lerch*[a]

Dedicated to Professor Hartmut Bärnighausen on the Occasion of His 80th Birthday

Keywords: Synthesis; Nickel; Cobalt; NMR spectroscopy; X-ray diffraction

Abstract. A new synthesis route to Li_2NiF_4 based on a fluorolytic process using $Ni(acac)_2$ or $Ni(OAc)_2{\cdot}4H_2O$ as precursor is presented. Variation of the synthesis conditions allows crystallite size control of the obtained powders. ^6Li and ^7Li MAS NMR experiments were carried out to study local environments of the lithium ions. Several attempts were made to synthesize Li_2CoF_4, which are, unfortunately, hitherto not successful. Nevertheless, our studies clearly reveal that solid solutions Li_2NiF_4–Li_2CoF_4 are stable up to ca. 30 % cobalt. High-temperature X-ray diffraction measurements also show no evidence for the existence of pure Li_2CoF_4. These findings are supported by quantum chemical calculations.

Introduction

In the last years fluorides have attracted increasing attention as cathode materials for lithium-ion batteries. Compounds of the Li_xMF_y-type, where M represents a transition metal, are distinguished by a high amount of lithium together with a variety of structural features and possible oxidation states of M. Some exponents of this class of materials, such as monoclinic Li_3FeF_6[1] and Li_3VF_6,[2] have already been electrochemically investigated. From a crystal chemistry point of view Li_2NiF_4 may also be considered to serve as a cathode material in lithium-ion batteries. Li_2NiF_4 crystallizes in the well-known inverse spinel-type structure (space group $Fd\bar{3}m$).[3,4] Usually, it is prepared by solid-state reaction of LiF and NiF_2 at 680 °C[3] or by high-pressure solvothermal synthesis carried out at 625 °C,[4] or by fluorination of $Li_2[Ni(CN)_4]$ with an additional heating procedure in vacuo.[5]

* Prof. Dr. M. Lerch
Fax: +49-30-31479656
E-Mail: martin.lerch@tu-berlin.de
[a] Technische Universität Berlin
Institut für Chemie, Sekr. C2
Straße des 17. Juni 135
10623 Berlin, Germany
[b] Mulliken Center for Theoretical Chemistry
Institut für Physikalische and Theoretische Chemie,
Universität Bonn
Beringstr. 4
53115 Bonn, Germany
[c] Institut für Chemische Technologie von Materialien
Technische Universität Graz
Stremayrgasse 9
8010 Graz, Austria
[d] Institut für Physikalische Chemie und Elektrochemie
Leibniz Universität Hannover
Callinstraße 3a
30167 Hannover, Germany

So far, this particular fluoride has also been in the focus of some electrochemical investigations. In 1999, the properties of an electrode made from Li_2NiF_4, graphite, and polyvinyldifluoride were investigated; the voltage (vs. Li metal) was reported to be 5.1 V.[6] Moreover, mixed spinels such as $Li_2Ni_{1-x}Co_xF_4$ are also of interest: As an example, a cathode utilizing $Li_2Ni_{0.8}Co_{0.2}F_4$ shows a voltage of 5.2 V (vs. lithium metal).[6] In contrast to Li_2NiF_4, only little information can be found in the literature concerning the existence of the cobalt counterpart Li_2CoF_4. To the best of our knowledge, there is only one single reference mentioning this compound; the possible phase formation of Li_2CoF_4 in the quasi binary system LiF–CoF_2 was investigated by means of X-ray powder diffraction and thermoanalytical methods (using Ni-containers!).[7] The authors observed a diffraction pattern being similar to that of the nickel analogue and concluded that Li_2CoF_4 had been formed. However, apart from that work the formation of Li_2CoF_4 has never been reported again.

Keeping in mind the potential use of these spinels as cathode materials, the high synthesis temperature reported (> 600 °C for Li_2NiF_4) is far away from being optimally suited to control the morphology. Unfortunately, large crystallite sizes, which unavoidably form at such high temperatures, turn out to be disadvantageous for electrochemical applications. This is because of the resulting large Li^+ and e^- diffusion lengths as well as the poor electronic conductivity of lithium transition metal fluorides, which calls for additives enhancing e^- transport. The present work aims at developing a new, low-temperature synthesis route for Li_2NiF_4 based on precursors synthesized from corresponding organic salts such as acetylacetonates and acetates, respectively. As mentioned above, Li_2NiF_4 is formed at 680 °C; it is only stable in a narrow temperature range, i.e.,

Zeitschrift für anorganische und allgemeine Chemie ZAAC Journal of Inorganic and General Chemistry

the reaction is incomplete below 680 °C and the product decomposes to the binary fluorides above this temperature. Recently we showed that, for example, Li_3VF_6 can be successfully prepared at low temperatures from LiO*t*Bu, $V(acac)_3$, and HF/EtOH by heating the precursor up to 300 °C only. This method is based on the fluorolytic sol-gel process described by *Kemnitz* et al.[8] The applicability of this route on fluorometalates has also been demonstrated by the same group.[9] The mean crystallite size of the powders could be modified by varying the decomposition temperature of the precursor.[10] In respect to this work, the intention of the presented study is to synthesize Li_2NiF_4 from LiO*t*Bu, $Ni(acac)_2$/$Ni(OAc)_2$, and various HF solutions with subsequent heating procedures of the precursors. Herein, main emphasis will be put on the decrease of the synthesis temperature as well as on the variation of the particle size. Additionally, our attempts on the preparation of pure Li_2CoF_4 and the solid solutions of the Ni- and Co-spinels ($Li_2Ni_{1-x}Co_xF_4$) will be presented as well.

Results and Discussion

Synthesis of Li_2NiF_4

Li_2NiF_4 can be synthesized via a two-step route. During the first step, $Ni(OAc)_2{\cdot}4H_2O$ or $Ni(acac)_2$ reacts with LiO*t*Bu and HF in an organic solvent. The precursor is obtained after the solvent was removed and the mixture was dried in vacuo. Heating the precursor in nitrogen atmosphere yields the desired spinel phase. The corresponding X-ray powder diffraction patterns of the precursors, which turned out to be mainly X-ray amorphous, only show broad reflections of LiF. Depending on the kind of organic solvent and the Ni-educt used, some samples contain traces of $NiSiF_6{\cdot}6H_2O$ and/or Li_2SiF_6 originating from the reaction of HF with the Schlenk tube. Only the use of ethanol results in powders free of crystalline silicon compounds.

In the following section the preparation of the spinel-type phase of Li_2NiF_4 is described, while main emphasis is put on the attempt to lower the synthesis temperature as compared to the routes described in the literature so far. $Ni(acac)_2$ precursors as well as $Ni(OAc)_2$-derived precursors were dried at 120 °C for 2 h and afterwards heated for 10 h at various temperatures ranging from 400 °C to 750 °C. Some significant differences are observed: the decomposition of the $Ni(acac)_2$ precursor led to the formation of Li_2NiF_4 as main phase even at 400 °C. Ni and LiF are detected as side phases (see Figure 1a).

In contrast to this observation, heating $Ni(OAc)_2$-derived precursors in the same way led to LiF/NiF_2 mixtures rather than to the formation of the spinel phase (Figure 2a). Increasing the decomposition temperature, the ratio Li_2NiF_4/LiF/Ni remains constant for the $Ni(acac)_2$ precursor between 500 °C and 680 °C. Finally, at 750 °C no nickel metal can be observed any longer. Again, the behavior of the $Ni(OAc)_2$ precursor is different: together with a small amount of LiF, the desired main phase Li_2NiF_4 forms at temperatures ranging from 500 °C to 750 °C (Figure 2). In addition, it was found that the formation of the spinel phase depends on the kind of organic solvent used for the preparation of the precursor (Figure 3). In

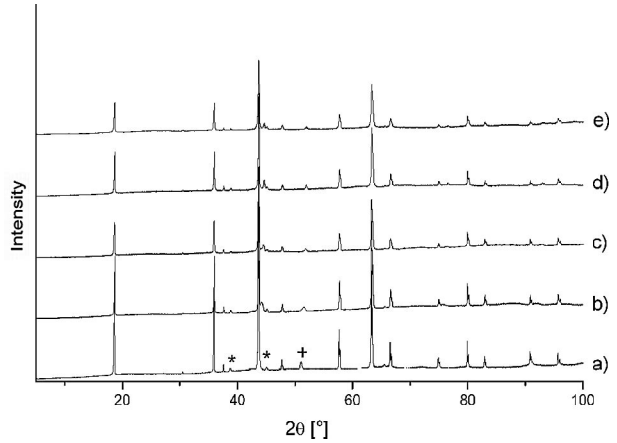

Figure 1. X-ray diffraction patterns of the powders obtained by heating $Ni(acac)_2$-based precursors for 10 h at different temperatures: (a) 400 °C: mixture of Li_2NiF_4, LiF, Ni; (b) 500 °C; (c) 600 °C; (d) 680 °C; (e) 750 °C: Li_2NiF_4 with small amounts of LiF (* mark the characteristic reflections of LiF, + marks nickel metal).

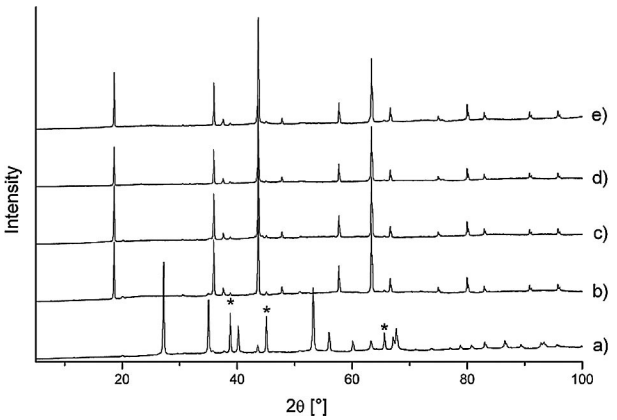

Figure 2. X-ray diffraction patterns of the powders obtained by heating $Ni(OAc)_2$-based precursors for 10 h at different temperatures: (a) 400 °C: mixture of NiF_2 and LiF; (b) 500 °C; (c) 600 °C; (d) 680 °C; (e) 750 °C: Li_2NiF_4 with small amounts of LiF (* mark the characteristic reflections of LiF).

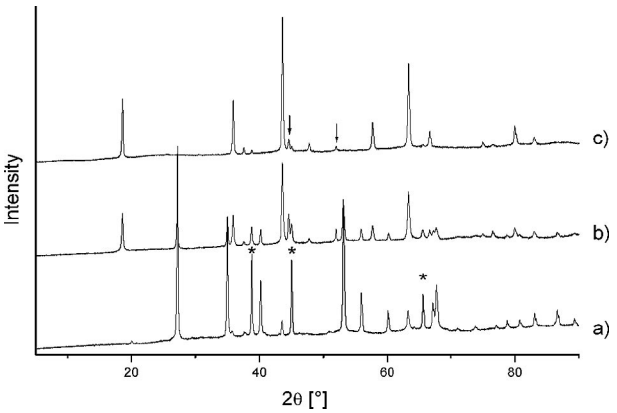

Figure 3. X-ray diffraction patterns of finally obtained powders using different organic solvents for precursor synthesis (decomposition for 10 h at 400 °C): (a) $Ni(OAc)_2$/EtOH: mixture of LiF and NiF_2; (b) $Ni(acac)_2/Et_2O$: Li_2NiF_4 with LiF, NiF_2, and Ni; (c) $Ni(acac)_2$/EtOH: Li_2NiF_4 with small amounts of LiF and Ni (* mark the reflections of LiF, arrows (↓) mark the reflections of Ni).

general, $Ni(acac)_2$/ethanol must be considered as first choice, only with ethanol as solvent Li_2NiF_4 is formed even at 400 °C.

The formation of Li_2NiF_4 was also investigated as function of the precursor decomposition time. Both the $Ni(OAc)_2$ precursor and the $Ni(acac)_2$-derived precursor were heated for 4 h, 40 h, and 100 h at 400 °C and 680 °C, respectively. It is worth noting that no significant differences of the ratio spinel phase / LiF were observed.

Bearing the properties of powerful cathode materials in mind, it might be crucial to control the crystallite size by, e.g., the variation of the decomposition temperature of the precursor. As an example, the effect of decomposition time on the resulting crystallite sizes was explicitly investigated at several temperatures (400 °C, 500 °C, 600 °C). Mean crystallite sizes were estimated from broadening of the X-ray powder reflections by using the formula introduced by Scherrer.[11] The results are summarized in the following. The mean crystallite sizes of Li_2NiF_4, synthesized by decomposition (t_d = 10 h) of the $Ni(acac)_2$ precursor, are 66 nm (400 °C), 98 nm (500 °C), and 106 nm (600 °C), respectively. Reducing the decomposition time t_d to 4 h led to a mean crystallite size of 55 nm at 400 °C. Further decrease of t_d (2 h) resulted in crystallites with a mean diameter of ca. 22 nm. REM measurements of powders prepared from $Ni(acac)_2$/EtOH at 400 °C (t_d = 2 h) exhibit particle sizes in a range of 150–200 nm. Such small nanoparticles are definitely of interest for cathode active materials in lithium ion batteries.[12,13]

Besides the characterization by X-ray powder diffraction, first ^7Li and ^6Li MAS NMR spectra were recorded to probe local environments of the Li spins in Li_2NiF_4.

To optimize phase purity of the samples and avoid the presence of amorphous phases the solid state route described in the literature[3] was chosen. The sample used for NMR investigations contains 98 % Li_2NiF_4 and approximately 2 % LiF. The crystal structure of Li_2NiF_4 can be described as inverse spinel type. This means a nominal distribution of Li in the following way: lithium ions fully occupy the tetrahedral 8*a* sites and share the octahedral sites 16*d* with Ni presumably in an irregular manner. Thus, half of the 16*d* sites are occupied by Ni according to the formula Li[Li,Ni]F_4. The 8*a* sites are surrounded by twelve 16*d* sites and are connected to these sites by corner sharing. Apart from the 8*a* sites in the direct neighborhood, each Li/Ni site is connected to six 16*d* sites by sharing a common edge of the surrounding 16*d* octahedra.[3,4] As a result of our Rietveld refinements, the used Li_2NiF_4 is not a real inverse spinel: ca. 10 % of the tetrahedral sites are occupied by nickel ions. This is also observed for the samples prepared by the fluorolytic route.

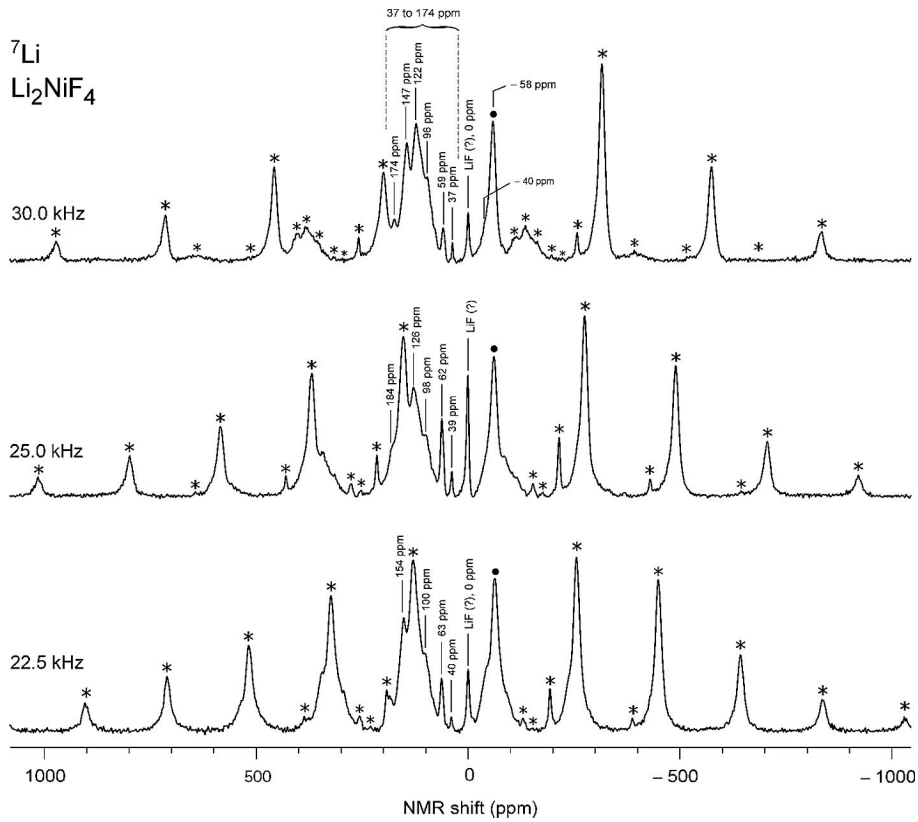

Figure 4. ^7Li MAS NMR spectra of Li_2NiF_4 recorded at 116 MHz and the rotation frequencies indicated. Although bearing gas at ambient temperature was used, spinning causes an increase of the temperature inside the NMR rotor. Thus, the Li NMR signals expectedly shift towards smaller ppm values due to Curie-Weiss behavior. Most of the spinning sidebands are marked with asterisks. As an example, at a rotation frequency of 30 kHz, the Li NMR signals range from 174 ppm to 37 ppm. Interestingly, an intense and rather broad NMR signal also shows up at negative ppm values. The isotropic line, marked by a circle (●), is located at –58 ppm (see also Figure 5) at a spinning frequency of 30 kHz and ambient bearing gas pressure.

Zeitschrift für anorganische und allgemeine Chemie ZAAC Journal of Inorganic and General Chemistry

In general, the Li NMR (paramagnetic) shift is influenced by the extent and kind of electron spin-density transferred from the nickel ions to the central lithium atoms.[14]

Due to the presumably irregular number of nickel ions residing in the neighborhood of the Li spins, the corresponding ^{7}Li MAS NMR spectrum is expected to show a distribution of NMR signals reflecting the various Fermi-contact hyperfine interactions of the Li spins with the paramagnetic central Ni^{2+} ions. Since the contact shift is additive, the NMR lines are expected to directly reflect the various numbers of Ni^{2+} ions in the neighborhood (first and second nearest neighbors) of the Li spins (see for example Refs [15,16]).

In Figure 4 some of the ^{7}Li MAS NMR spectra of Li_2NiF_4 are shown. The spectra were recorded at different spinning frequencies in order to differentiate between spinning sidebands, shifting with the rotation frequency, and the (isotropic) NMR lines being of interest. While the signal near 0 ppm most likely represents a diamagnetic impurity such as LiF (vide supra), at a rotation speed of 30 kHz distinct NMR lines show up whose shifts range from 174 ppm to 37 ppm. In contrast to the signal near 0 ppm, they shift towards larger ppm values the smaller the spinning frequency is chosen. Such a dependence reflects Curie-Weiss behavior because the larger the spinning frequency the higher the temperature inside the NMR rotor, which simply stems from the effect of friction (MAS effect). It is worth mentioning that the NMR lines appear in an almost equidistant manner. Probably, this directly reflects the number of central nickel atoms in the coordination sphere of lithium (see also Refs [15,16]).

Interestingly, besides these NMR intensities a relatively broad Li NMR signal shows up, which is characterized by a negative contact shift. By using ^{6}Li MAS NMR, carried out at a spinning speed of 65 kHz, we were able to identify the associated isotropic line being located at approximately –60 ppm (see Figure 5).

In general, ^{6}Li NMR measurements[16] take advantage of the small magnetogyric ratio $\gamma(^6\text{Li})$; moreover, the ^{6}Li nucleus is exposed to rather small second order quadrupole interactions, which might additionally affect the shape of ^{7}Li MAS NMR spectra. In the case of ^{7}Li (and at a spinning speed of 30 kHz, Figure 4) the isotropic signal of the broad NMR intensity is located at –58(2) ppm; it shifts only slightly with temperature.

The intensity near –40 ppm (see, for example the ^{7}Li NMR spectra recorded at 30 kHz and 22.5 kHz, respectively, of Figure 4) might indicate an additional NMR signal of very low intensity being also characterized by a negative contact shift. It also shows up in the corresponding ^{6}Li MAS NMR spectrum recorded at 65 kHz (Figure 5). It is worth mentioning that the NMR line at 0 ppm is characterized by a ^{6}Li NMR spin-lattice relaxation time, $T_1 > 200$ ms, which is much larger than those of the other NMR lines ($T_1 < 3$ ms). This further supports the assumption that the line at 0 ppm belongs to a diamagnetic impurity rather than to lithium ions in Li_2NiF_4.

In the most general sense, the transfer of positive electron spin density to the 2s orbital of the lithium ions will lead to an additive local field resulting in a shift towards positive ppm values. On the other hand, the transfer of negative spin density will lead to negative shifts as indeed observed in the present case.[14,17] The final (total) Fermi contact shift is either dominated by a specific transfer mechanism or represents the result of a combination of different spin transfer effects such as delocalization of spin density or polarization of spin orbitals.[14,17–22] Considering the spin configuration of Ni^{2+}(d8), which is $t_{2g}^6e_g^2$, the unpaired electrons might polarize the doubly occupied t_{2g} crystalline orbitals. In the case of a 90° *M*–F–Li interaction this would lead to an increase of positive spin density at the transition metal, while negative spin density is induced on the fluorine (p) and lithium (s) orbitals (polarization of the t_{2g}–p_π–s orbitals).[14] The transfer of positive spin density can occur via an 180° *M*–F–Li interaction involving the p_σ fluorine orbitals. However, there are no 180° *M*–F–Li angles in Li_2NiF_4, which also seems to rule out other transfer mechanisms[14] needing such arrangements and involving e_g orbitals. Here, the transfer of negative spin density might indeed be possible via 90° *M*–F–Li interactions in Li_2NiF_4. Nickel ions residing on tetrahedral sites, as indicated above, might also be responsible for negative ppm shifts because the loops of the t_2 orbitals present in tetrahedral coordination of a Ni^{2+} ion roughly point into the direction of a lithium ion in an adjacent octahedral site.[23]

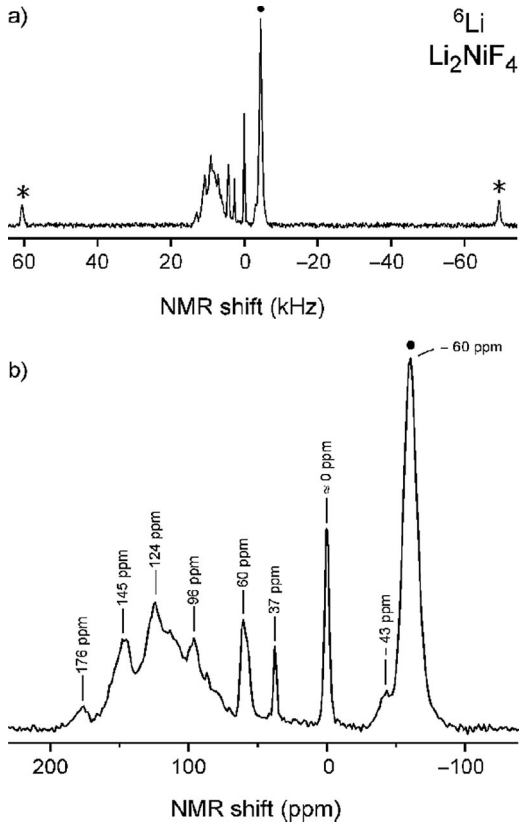

Figure 5. (a) ^{6}Li MAS NMR spectrum of Li_2NiF_4 recorded at 65 kHz (ambient bearing gas temperature) using a 1.3-mm rotor. Due to the high spinning frequency the sideband manifold (asterisks) is largely reduced. (b) Magnification of the spectrum shown in (a). The ppm values of the most intense NMR lines are indicated. Whereas the intensity at ≈0 ppm is characterized by a spin-lattice relaxation time T_1 of approximately 200 ms, for the other signals, $T_1 < 3$ ms is found indicating that the signal at 0 ppm most likely represents a diamagnetic impurity. See text for further explanation.

Dedicated Issue

Attempts to Synthesize Li_2CoF_4

In this part various attempts to synthesize Li_2CoF_4 are presented, following the successful routes to Li_2NiF_4.

(1) Precursor Decomposition as Described above for Li_2NiF_4

$Co(OAc)_2{\cdot}4H_2O$ was used as starting material. The obtained precursor was heated under various conditions in analogy to the successful nickel spinel routes. Unfortunately, in all experiments mixtures of LiF and CoF_2 were obtained. No indications for the formation of Li_2CoF_4 are observed, not even smallest reflections of this phase are found in the X-ray diffraction patterns. In addition, the possibility to form solid solutions $Li_2Ni_{1-x}Co_xF_4$ was evaluated by the precursor route. To summarize the results, up to approximately 25% cobalt can be incorporated into the spinel phase, resulting in ~$Li_2Ni_{0.75}Co_{0.25}F_4$.

(2) Reaction of Hydrofluoric Acid with Carbonates

It has long been known that metal fluorides can be synthesized by the reaction of metal carbonates with hydrofluoric acid.[24] Thus, Li_2CO_3, $NiCO_3$, $CoCO_3$, and overstoichiometric amounts of HF (40 wt%) were used to prepare various compounds of $Li_2Ni_{1-x}Co_xF_4$ with $0 < x < 1$. After removing the liquid components, mixtures of LiF and $(Ni,Co)F_2{\cdot}4H_2O$ were obtained. These mixtures were heated for 10 h at 640 °C and 680 °C, respectively. Apparently, for $0 < x < 0.3$, cobalt is incorporated in the spinel phase (see Table 1). This is reflected by the variation of the lattice parameter *a*, which increases with the amount of cobalt incorporated (see Table 2). For all samples Rietveld refinements reveal significant amounts of LiF as side phase. Besides that also small contents of $(Ni,Co)F_2$, nickel cobalt oxide (Ni,Co)O and a Ni-type phase (Ni/Co) were formed. Surprisingly, the reduction to metal and the formation of monoxides (from the presence of hydrate water) occurs.

The lattice parameters of the difluorides show the same tendency as for the $Li_2Ni_{1-x}Co_xF_4$ phases. The parameters *a* and *c* steadily increase with increasing amounts of cobalt. For comparison, the refined values are listed in Table 2. For $0.4 < x < 0.6$ and also higher contents of cobalt the amount of the spinel phase decreases drastically leading to the main presence of $(Ni,Co)F_2$ and LiF. No spinel phase is formed at $x \geq 0.7$. In good agreement with the results of the precursor route, the maximum amount of cobalt, which can be incorporated in the spinel phase is approximately $x = 0.3$, leading to ~$Li_2Ni_{0.7}Co_{0.3}F_4$.

(3) Solid-State Route using LiF/CoF_2 Mixtures

As mentioned in the introduction, the formation of Li_2CoF_4 by heating mixtures of LiF and CoF_2 up to approximately 650 °C was reported.[7] The authors investigated the phase diagram of the quasi binary LiF–CoF_2 system by using thermoanalytical methods combined with *ex situ* X-ray powder diffraction measurements carried out after cooling the samples. In the presented phase diagram the stability range of the spinel-type phase ranges from 606 °C to 670 °C. This phase was also observed by the authors when a mixture of 10 mol-% CoF_2 and 90 mol-% LiF was used. Following these results, four different mixtures of CoF_2 and LiF were reacted in the temperature range between 600 °C and 700 °C. The amount of CoF_2 was chosen to be 10, 25, 33.3, and 50 mol-%, respectively. A content of 33.3 mol-% CoF_2 represents the "spinel-type" mixture LiF:CoF_2 = 2:1. Independent of composition, temperature, and heating time, our experiments show that no spinel phase does form. In all experiments only mixtures of LiF and CoF_2 were

Table 1. Observed phases for the carbonate route used to prepare $Li_2Ni_{1-x}Co_xF_4$.

Theoretical composition $Li_2Ni_{1-x}Co_xF_4$	Phases obtained after drying	Phases obtained after the heating procedure at 640 °C
$x = 0$	$NiF_2{\cdot}4H_2O$, LiF	Li_2NiF_4 (81%), LiF (9%), NiO (8%), NiF_2 (2%)
$x = 0.1$	$(Ni,Co)F_2{\cdot}4H_2O$, LiF	~ $Li_2Ni_{0.9}Co_{0.1}F_4$ (87%), LiF (6%), (Ni,Co)O (6%), $(Ni,Co)F_2$ (1%)
$x = 0.2$	$(Ni,Co)F_2{\cdot}4H_2O$, LiF	~ $Li_2Ni_{0.8}Co_{0.2}F_4$ (92%), LiF (3%), Ni,Co (3%), $(Ni,Co)F_2$ (2%)
$x = 0.3$	$(Ni,Co)F_2{\cdot}4H_2O$, LiF	~ $Li_2Ni_{0.7}Co_{0.3}F_4$ (73%), LiF (17%), Ni,Co (1%), $(Ni,Co)F_2$ (9%)
$x = 0.4$	$(Ni,Co)F_2{\cdot}4H_2O$, LiF	"~ $Li_2Ni_{0.72}Co_{0.28}F_4$"[a] (14%), LiF (37%), $(Ni,Co)F_2$ (49%)
$0.5 < x < 0.6$	$(Ni,Co)F_2{\cdot}4H_2O$, LiF	$Li_2Ni_{1-x}Co_xF_4$ (traces), $(Ni,Co)F_2$, LiF
$0.7 < x < 0.9$	$(Ni,Co)F_2{\cdot}4H_2O$, LiF	$(Ni,Co)F_2$, LiF
$x = 1$	$CoF_2{\cdot}4H_2O$, LiF	CoF_2, LiF

a) Stoichiometry calculated from the determined lattice parameter.

Table 2. Lattice parameters of solid solutions $Li_2Ni_{1-x}Co_xF_4$ and $(Ni,Co)F_2$ phases with $0 < x < 0.4$.

Theoretical composition $Li_2Ni_{1-x}Co_xF_4$	Spinel phases	Rutile-type difluorides
$x = 0$	Li_2NiF_4: a = 831,76(1)	NiF_2: a = 465,58(4), c = 308,40(3)
$x = 0.1$	~ $Li_2Ni_{0.9}Co_{0.1}F_4$: a = 832,24(1)	$(Ni,Co)F_2$: a = 466,05(3), c = 309,69(5)
$x = 0.2$	~ $Li_2Ni_{0.8}Co_{0.2}F_4$: a = 833,23(1)	$(Ni,Co)F_2$: a = 466,46(4), c = 310,99(5)
$x = 0.3$	~ $Li_2Ni_{0.7}Co_{0.3}F_4$: a = 833,96(2)	$(Ni,Co)F_2$: a = 467,16(2), c = 312,20(2)
$x = 0.4$	$Li_2Ni_{1-x}Co_xF_4$: a = 833,78(5)	$(Ni,Co)F_2$: a = 467,52(2), c = 312,83(1)

obtained – even when heating times as long as 120 h were chosen. For a more detailed investigation and for comparison with the results obtained for the LiF–NiF_2 system, in situ high-temperature X-ray diffraction measurements were carried out at temperatures up to 750 °C using "spinel-type" mixtures of LiF/NiF_2 and LiF/CoF_2 (LiF:MF_2 = 2:1). In addition, also the LiF/CoF_2 mixture containing 10 mol-% CoF_2, emphasized in the literature,[7] was investigated. In Figure 6 the results obtained for the LiF/NiF_2 mixture are depicted. At approximately 500 °C reflections of spinel-type Li_2NiF_4 are clearly observed. Above 700 °C an almost single spinel phase is present. This result is in good agreement with that presented in the literature.[3] A completely different behavior is observed for the corresponding Co-containing mixtures (see Figure 7). Independent of temperature, the experiments reveal no indications pointing to the formation of a spinel phase. The reflections of LiF strongly shift towards lower 2θ values at ~ 600 °C, indicating a significant solubility of CoF_2 in LiF at elevated temperatures. In the temperature range from 680 °C to 700 °C the intensities of the CoF_2 reflections decrease dramatically. At higher temperatures the formation of Co_2SiO_4 starts, which originates from the reaction of Co-containing phases with the SiO_2 capillary. Similar results were obtained for the mixture containing 10 mol-% CoF_2.

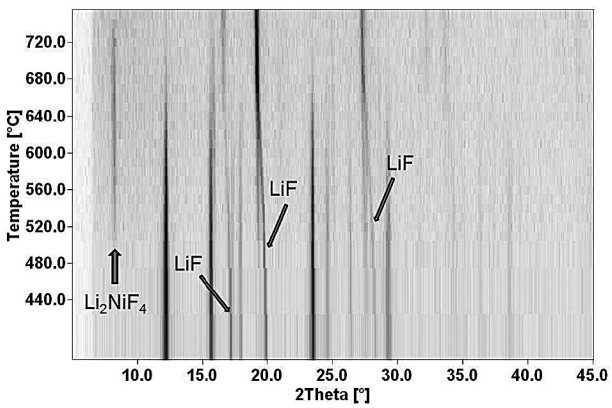

Figure 6. In situ high-temperature X-ray diffraction measurements of a mixture of LiF and NiF_2 (LiF:NiF_2 = 2:1). Up to 520 °C, LiF and NiF_2 exist. At approximately 500 °C the formation of Li_2NiF_4 starts. At ca. 700 °C mainly Li_2NiF_4 is observed.

Quantum-Chemical Calculations

The thermodynamic stability of $Li_2Ni_{1-x}Co_xF_4$ (x = 0, 0.125, 0.25, 0.5, 1) was studied theoretically at density-functional theory (DFT) level. Based on our experience with open-shell transition metal compounds[25] we used the DFT-Hartree-Fock hybrid functional PW1PW.[26] The calculations were performed with the crystalline-orbital program package CRYSTAL09.[27] Atomic basis sets of triple-zeta quality for the elements Li, Ni, Co, and F were taken from the CRYSTAL homepage[28] and augmented with diffuse shells and polarization functions. A detailed description of the optimized solid-state basis sets will be given elsewhere.[29] The cobalt mole fraction x was varied by changing the size of the unit cell correspondingly. In the mixed phases we started with composition Li_2NiF_4 and replaced one Ni by Co. In this way only highly ordered Ni/Co distributions were considered in order to reduce the computational effort. Possible clustering effects were ignored, which can affect the calculated reaction energies. The presented results should therefore only be regarded as semi-quantitative, but are expected to reproduce qualitative trends. Cell parameters and atomic positions of all cells were fully optimized. The thermodynamic functions at 300 K and 1000 K were calculated from the phonon frequencies obtained within the quasi-harmonic approximation.[30] In Table 3 the calculated free energies for the decomposition of the pure compounds Li_2NiF_4 and Li_2CoF_4 into the binary fluorides are presented. Under standard conditions (here we used 300 K instead of 298.15 K) Li_2NiF_4 is stable with respect to decomposition, while Li_2CoF_4 is not. This is in line with the experimental results of the presented study (vide supra). At elevated temperatures (we used 1000 K to approximate the experimental conditions) both Li_2MF_4 compounds are stabilized due to entropy effects. Li_2CoF_4 may be formed in a solid-state reaction at 1000 K and above, but will decompose during cooling.

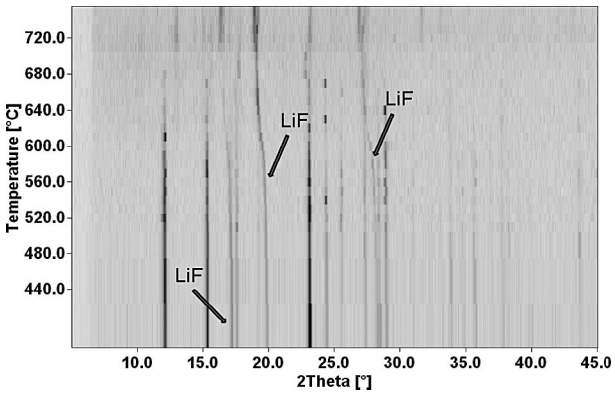

Figure 7. In situ high-temperature X-ray diffraction measurements of a "spinel-type" mixture of LiF and CoF_2 (LiF:CoF_2 = 2:1). At ca. 700 °C the formation of Co_2SiO_4 is observed.

Table 3. Calculated free energies ΔG /kJ·mol^{-1} for the reaction 2LiF + MF_2 → Li_2MF_4 (M = Ni, Co) as a function of temperature T /K.

T /K	300	1000
ΔG /kJ·mol^{-1}		
Li_2NiF_4	–11	–32
Li_2CoF_4	+5	–3

With the unit cells and the theoretical approach described above we calculated the free energy of the reaction

$$2LiF + (1–x)NiF_2 + xCoF_2 \rightarrow Li_2Ni_{1-x}Co_xF_4 \quad (1)$$

for x = 0.125, 0.25, and 0.5. In Figure 8 the results are shown for T = 1000 K. At this temperature incorporation of up to 25 % cobalt leads to stable compounds with ΔG between –32 kJ·mol^{-1} (x = 0) and –20 kJ·mol^{-1} (x = 0.25). At x = 0.5 the situation has changed drastically, ΔG being highly positive (+60 kJ·mol^{-1}).

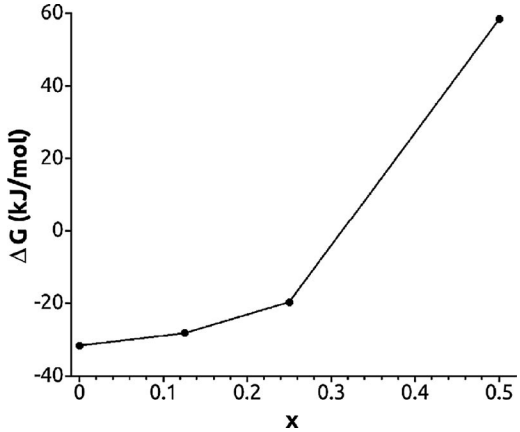

Figure 8. Calculated free energy ΔG /kJ·mol^{-1} at 1000 K for the formation of $Li_2Ni_{1-x}Co_xF_4$ from the binary fluorides as a function of x.

A simple linear interpolation indicates that ΔG changes sign for $x = 0.3$ to $x = 0.4$. Again, this is in line with the experimental findings of the presented study.

From our experimental findings and the presented calculations the reported existence of Li_2CoF_4[7] must be called into question. Unfortunately, the authors of reference[7] have not presented refined lattice parameters. This leads to severe problems taking into account the container material used for the thermoanalytical measurements, which was nickel. Only a careful chemical analysis or determination of the lattice parameter of the spinel phase can avoid confusion. However, concerning this point no data is presented. If some nickel of the container material was involved in the reaction, the formation of a mixed spinel phase $Li_2Ni_{1-x}Co_xF_4$ is not astonishing.

Conclusions

A new precursor route being highly useful to prepare spinel-type Li_2NiF_4 was developed. The thermal decomposition of the precursors, synthesized from $Ni(acac)_2$, LiO*t*Bu, and HF in ethanol, for example, allows the decrease of the preparation temperature down to 400 °C. By variation of the temperature and the synthesis time the crystallite size can easily be optimized so that even nm-sized crystallites are obtainable. Expectedly, the preliminary ^{7}Li and ^{6}Li MAS NMR results reveal rather complex spectra, which is due to the various environments the lithium spins are exposed to in $Li[Li,Ni]F_4$. Additional 2D ^{6}Li MAS NMR spectra might be helpful to interpret the NMR paramagnetic shifts observed. The synthesis of the corresponding cobalt spinel phase Li_2CoF_4 turned out to be not successful. This result is independent from the particular route chosen, i.e., preparation via acetylacetonates/alcoholates, by employing carbonates, or by solid-state reaction. So far, our experimental studies do not give any indication for the existence of Li_2CoF_4. This is supported by quantum-chemical calculations of the corresponding free energies at density-functional level. However, on the other hand cobalt can be present in spinel-type solid solutions up to the composition of ~$Li_2Ni0_{.7}Co_{0.3}F_4$, which is in excellent agreement with the calculations presented.

Experimental Section

Materials and Methods: $Ni(acac)_2$, CoF_2 (ABCR), $CoCO_3$, $NiCO_3$, Li_2CO_3 (Alfa Aesar), $Ni(OAc)_2{\cdot}4H_2O$, $Co(OAc)_2{\cdot}4H_2O$, LiO*t*Bu, hydrofluoric acid (40 wt-%), and LiF (Sigma-Aldrich) were used as received. HF solutions in ethanol, THF, and Et_2O were prepared by feeding gaseous HF into the solvent under cooling. The solvents were dried using standard literature procedures. All reactions were carried out by using standard Schlenk techniques. Reagents and samples were stored in a glove box in an argon atmosphere.

General Synthesis

Synthesis of the Li_2NiF_4-Precursor: $Ni(acac)_2$ (1 g, 3.89×10^{-3} mol) (alternatively $Ni(OAc)_2{\cdot}4H_2O$) and LiO*t*Bu (0.6232 g, 7.79×10^{-3} mol) (Li:Ni = 2:1) were weighed into a Schlenk tube and suspended in absolute ethanol (30 mL) at room temperature. To the resultant suspension HF-EtOH solution (6.25 mL, 12.50 M) was added, leading to a light green solution (Ni:HF = 1:20). Alternatively, a HF-Et_2O (6.76 M) or a HF-THF (0.68 M) solution was used. The solutions were stirred 2 h at room temperature. Afterwards, the solvent was removed in a vacuum and the fine green powder was dried for 2 h at 80 °C.

Synthesis of Li_2MF_4: All syntheses were carried out in sealed copper capsules in a nitrogen atmosphere. The respective precursor (ca. 100–200 mg) was filled into a one-side mechanically sealed capsule, which was afterwards completely closed. If not described else wise, all samples were slowly cooled down to ambient temperature.

Elemental Analysis: The carbon and hydrogen contents were determined by combustion analysis (Thermo Finnigan FlashEA 1112 NC analyzer), the oxygen contents with a LECO EF-TC 300 N_2/O_2 analyzer (hot gas extraction). The carbon, hydrogen, and oxygen contents of the precursor samples and of the Li_2NiF_4 samples vary with the Ni-educt and solvent used for precursor synthesis. The following amounts (wt-%) of C, H, and O were detected: $Ni(OAc)_2/Et_2O$: C 1.9, H 2.6, O 22 %; $Ni(OAc)_2$/EtOH: C 4.0, H 2.3, O 16 %. For Li_2NiF_4-precursors based on $Ni(acac)_2$, the values of C and H are considerably higher: $Ni(acac)_2/Et_2O$: C 7.3, H 2.4, O 13 %. Precursors based on $Ni(acac)_2$/EtOH exhibit the highest carbon contents, oxgen contents are the same as for the system with Et_2O: C 9.5, H 2.6, O 12 %. Li_2NiF_4 samples prepared by decomposition of $Ni(OAc)_2$/EtOH precursors contain 0.2–0.3 % carbon and 0–0.1 % hydrogen. After decomposition at 400 °C, 1.4 % oxygen were measured. At higher temperatures, e.g. 680 °C, samples contained 0.7 % oxygen. Carbon contents of samples prepared from $Ni(acac)_2$/EtOH-precursors range between 0.4–0.7 %, hydrogen contents range between 0–0.05 %. Samples prepared by decomposition at 400 °C contained 0.9–1.3 % oxygen, at 680 °C 0.2–0.3 % oxygen are contained. Samples synthesized for MAS NMR measurements by the solid state route contained $<$ 0.06 % oxygen.

X-ray Powder Diffraction: X-ray powder diffraction measurements were performed with Cu-K_α radiation over a 2θ range from 5 to 120° (40 kV / 40 mV, Bragg-Brentano geometry, θ-θ arrangement). A PANalytical X′Pert PRO MPD diffractometer with PIXcel detector (Si-Li-semiconductor with 255 measuring channels) was used. Samples were prepared on small Si-cavity mounts. The program package FULLPROF 2009[31] was used for Rietveld refinements; peak profiles were fitted with a pseudo-Voigt function. In situ high-temperature XRD measurements were carried out with a STOE STADI-P diffractometer equipped with a graphite-heated resistance furnace (Mo-K_α radiation, λ = 70.93 pm, imaging plate detector, samples in SiO_2-glass capillaries in a nitrogen atmosphere).

^{7}Li Solid-State NMR: High-resolution solid-state NMR spectra were recorded with Avance III spectrometers (Bruker) connected to shimmed 7 Tesla and 11.4 Tesla cryomagnets. The resonance frequency was 116 MHz (^{7}Li) and 73 MHz (^{6}Li), respectively. Standard magic angle spinning (MAS) NMR probes (Bruker) in combination with 2.5-mm rotors (^{7}Li) and 1.3-mm rotors (^{6}Li) were used. The maximum spinning frequency accessible was 30 kHz (^{7}Li) and 65 kHz (^{6}Li), respectively. Spectra were acquired at ambient bearing gas temperature using a single pulse experiment; the excitation pulse length ranged from 1 to 2.15 µs. Fourier transformation, phasing and baseline correction of the data were carried out using Mnova software (Mestrelab Research). Line specific NMR spin-lattice relaxation times (T_1) were measured using the conventional saturation recovery pulse sequence.

Acknowledgements

We thank the German Ministry of Education and Research (BMBF) for financial support within the LIB 2015 initiative, project HE-Lion. *M. W.* and *P. H*. also acknowledge financial support by the DFG within the Research Unit 1277 "molife" We further thank *Prof. Erhard Kemnitz*, Humboldt University Berlin, Germany, for supplying the HF solutions.

References

[1] E. Gonzalo, A. Kuhn, F. Garcia-Alvarado, *J. Power Sources* **2010**, *195*, 4990.
[2] I. Gocheva, K. Chihara, S. Okada, J. Yamaki, Lithium Batteries Discussion 2011 – Electrode Materials – Arcachon, France (extended abstract).
[3] W. Rüdorff, J. Kändler, D. Babel, *Z. Anorg. Allg. Chem.* **1962**, *317*, 261.
[4] J.-L. Fourquet, H. Duroy, M. Leblanc, G. Ferey, *J. Solid State Chem.* **1989**, *78*, 184.
[5] W. Rudorff, J. Kandler, *Naturwissenschaften* **1957**, *44*, 418.
[6] Komiya, Hirokazu; Nitta, Yoshiaki; Okamura, Kazuhiro, Secondary Nonaqueous Electrolyte Batteries, *Jpn. Kokai Tokkyo Koho* **1999**, JP 11339800 A 19991210 (Patent).
[7] L. A. Ol'khovaya, M. B. Ikrami, T. A. Nikolaeva, I. Y. Gracheva, *Russ. J. Inorg. Chem.* **1989**, *34*, 566.
[8] E. Kemnitz, U. Groß, S. Rüdiger, C. S. Shekar, *Angew. Chem. Int. Ed.* **2003**, *42*, 4251.
[9] M. Ahrens, G. Scholz, M. Feist, E. Kemnitz, *Solid State Sci.* **2006**, *8*, 798–806.
[10] J. Kohl, D. Wiedemann, S. Nakhal, P. Bottke, N. Ferro, T. Bredow, E. Kemnitz, M. Wilkening, P. Heitjans, M. Lerch, *J. Mater. Chem.* **2012**, *22*, 15819.
[11] T. Ressler, *WINXAS v3.1* **2011**.
[12] P. G. Bruce, B. Scrosati, J.-M. Tarascon, *Angew. Chem. Int. Ed.* **2008**, *47*, 2930.
[13] A. S. Aricò, P. Bruce, B. Scrosati, J.-M. Tarascon, W. V. Schalkwijc, *Nat. Mater.* **2005**, *4*, 366.
[14] D. Carlier, M. Ménétrier, C. P. Grey, C. Delmas, G. Ceder, *Phys. Rev. B* **2003**, *67*, 174103.
[15] C. Marichal, J. Hirschinger, P. Granger, M. Ménétrier, A. Rougier, C. Delmas, *Inorg. Chem.* **1995**, *34*, 1773.
[16] D. Carlier, M. Ménétrier, C. Delmas, *J. Mater. Chem.* **2001**, *11*, 594.
[17] C. Chazel, M. Ménétrier, L. Croguennec, C. Delmas, *Magn. Reson. Chem.* **2005**, *43*, 849.
[18] M. Wilkening, E. Romanova, S. Nakhal, D. Weber, M. Lerch, P. Heitjans, *J. Phys. Chem. C* **2010**, *114*, 19083.
[19] C. P. Grey, N. Dupré, *Chem. Rev.* **2004**, *104*, 4493.
[20] L. S. Cahill, R. P. Chapman, J. F. Britten, G. R. J. Goward, *J. Phys. Chem. B* **2006**, *110*, 7171.
[21] L. J. M. Davis, I. Heinmaa, G. R. Goward, *Chem. Mater.* **2010**, *22*, 769.
[22] L. S. Cahill, Y. Iriyama, L. F. Nazar, G. R. Goward, *J. Mater. Chem.* **2010**, *20*, 4340.
[23] A. R. Armstrong, C. Lyness, M. Ménétrier, P. G. Bruce, *Chem. Mater.* **2010**, *22*, 1892.
[24] A. Kurtenacker, W. Finger, F. Hey, *Z. Anorg. Allg. Chem.* **1933**, *211*, 83.
[25] M. M. Islam, T. Bredow, A. Gerson, *ChemPhysChem* **2011**, *12*, 3467.
[26] T. Bredow, A. R. Gerson, *Phys. Rev. B* **2000**, *61*, 5194.
[27] R. Dovesi, R. Orlando, B. Civalleri, C. Roetti, V. R. Saunders, C. M. Zicovich Wilson, *Z. Kristallogr.* **2005**, *220*, 571.
[28] http://www.crystal.unito.it/Basis_Sets.
[29] N. Ferro, C. Reimann, T. Bredow, in preparation.
[30] F. Pascale, C. M. Zicovich-Wilson, F. Lopez Gejo, B. Civalleri, R. Orlando, R. Dovesi, *J. Comput. Chem.* **2004**, *25*, 888.
[31] T. Roisnel, J. Rodriguez-Carvajal, *Mater. Sci. Forum* **2001**, *378–381*, 118.

Received: October 10, 2012
Published Online: December 18, 2012

Dedicated Issue

